

OTIC FILE COPY

2

FTD-ID(RS)T-0574-89

AD-A213 953

## FOREIGN TECHNOLOGY DIVISION

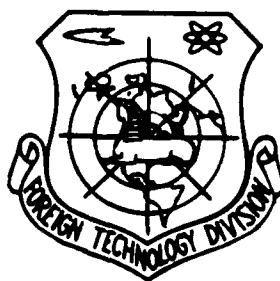


OCT 3 1989  
D 3

A NEW KIND OF HETERODYNE FIBER-OPTIC GYROSCOPE

by

Peng Gangding, Huang Shangyuan, Lin Zhongqi



Approved for public release;  
Distribution unlimited.

89 10 24 062

## HUMAN TRANSLATION

FTD-ID(RS)T-0574-89

23 August 1989

MICROFICHE NR: FTD-89-C-000713

A NEW KIND OF HETERODYNE FIBER-OPTIC GYROSCOPE

By: Peng Gangding, Huang Shangyuan, Lin Zhongqi

English pages: 8

Source: Guangxue Xuebao, Vol. 7, Nr. 7, July 1987,  
pp. 662-666

Country of origin: China

Translated by: SCITRAN

F33657-84-D-0165

Requester: FTD/TQTR/J.M. Finley

Approved for public release; Distribution unlimited.

THIS TRANSLATION IS A RENDITION OF THE ORIGINAL FOREIGN TEXT WITHOUT ANY ANALYTICAL OR EDITORIAL COMMENT. STATEMENTS OR THEORIES ADVOCATED OR IMPLIED ARE THOSE OF THE SOURCE AND DO NOT NECESSARILY REFLECT THE POSITION OR OPINION OF THE FOREIGN TECHNOLOGY DIVISION

PREPARED BY:

TRANSLATION DIVISION  
FOREIGN TECHNOLOGY DIVISION  
WPAFB OHIO

# GRAPHICS DISCLAIMER

All figures, graphics, tables, equations, etc. merged into this translation were extracted from the best quality copy available.

Accession No.	
NTIS GRA&I	<input checked="" type="checkbox"/>
DTIC TAB	<input type="checkbox"/>
Unannounced	<input type="checkbox"/>
Justification	
By	
Distribution/	
Availability Codes	
Dist	Availability or Special
A-1	



# A NEW KIND OF HETERODYNE FIBER-OPTIC GYROSCOPE

Peng Gangding, Huang Shangyuan, Lin Zhongqi

Abstract: In this paper a novel fiber-optic heterodyne detection technique of rotation rate is described. Using electro-optic frequency and highly birefringent single-mode fiber, the heterodyne fiber-optic gyroscope system no more needs the use of acousto-optic devices and is free from the direct current drift in the electronics. In addition, the reciprocity of the optical path in the system is improved. Preliminary experiments have shown a good linearity of the scale factor.

## 1. Introduction

Fiber-optic heterodynes have attracted great attention because they have a good linearity of the scale factor within a great dynamic range as well as simplicity of signal processing. The previously reported fiber-optic heterodyne techniques [1,2] have certain nonreciprocity of the optical path and need the use of acousto-optic frequency shifters which causes some problem of the system. Jackson, et al. [3] proposed the fiber-optic gyroscope configuration with highly birefringent fiber-optics for a polarization mode selection which improved the reciprocity of the optical path. However, it is a direct signal detector system which is easily affected by the direct-current drift in electronics. It is not as easy in signal processing and its sensitivity is not as high as the heterodyne system is. Besides, its linearity of the scale factor is not satisfactory.

This paper introduces a novel fiber-optic heterodyne gyroscope by applying the ordinary rotating wave plate technique in optical interference heterodyne systems [4-7] to highly birefringent fibers. Due to the behavior of polarization retention

of highly birefringent fibers, this configuration ensures system stable output in a polarization mode selection when needed by the rotating wave plate technique. It endows the system with good reciprocity and without the need of using acousto-optic devices. The heterodyne detection technique eliminates the direct-current drift in the electronics.

However, a rotating wave plate causes mechanical disturbances in the system. Besides, it is difficult to build a small-sized and solid-state system. According to Kaminov, et al. [8] and Buhrer, et al. [9], we have designed electro-optic frequency shifters made of  $\text{LiNbO}_3$  crystals, a crystal with triad symmetry, which can be replaced equivalently in an external rotating electrical field for mechanical rotating wave plates.

## 2. Fiber-optic heterodyne using rotating wave plate technique

Using the rotating wave plate technique, the direct-direction fiber-optic gyroscope reported in the literature [3] can be modified to a novel fiber-optic heterodyne gyroscope as shown in Figure 1. The circuit part above the dotline is the same as in the literature [3], but the part below the dotted line has been added to the new configuration. We performed heterodyne detection in polarization mode selection using electric-optic frequency shifters. Going through polarizer  $P_1$  with polarizing angle  $45^\circ$  from a horizontal direction, the beam from a laser source is split by the polarizing beam splitter PBS into two perpendicular polarized beams--horizontal and vertical which couple and enter into the fiber at the two ends of highly birefringent fibers. End A of fiber has been turned  $90^\circ$  from end B. Therefore, after entering the fiber at two ends, the two perpendicular linearly polarized beams can excite only the same polarization eigen mode. This is the so-called polarization mode selection using the behavior of polarization retention of highly birefringent fibers which enable the clockwise directional (CW) wave entering fiber at end A to come out at end B as a horizontal polarized beam and

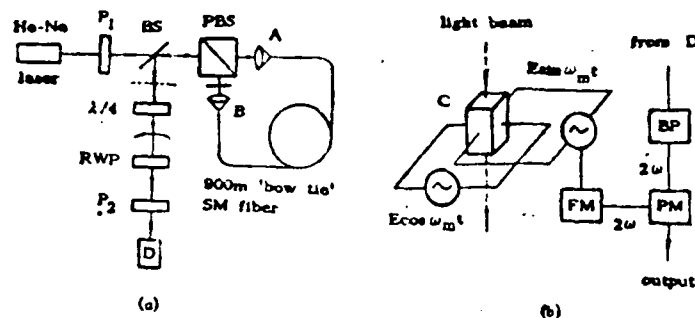


Fig. 1 Schematic diagrams of the gyroscope configuration  
 (a) Using a rotating wave plate as its frequency shifter. BS, beam splitter; PBS, polarization selective beam splitter;  $P_1$ , polarizer;  $P_2$ , analyzer; D, detector;  
 (b) Using a LiNbO<sub>3</sub> crystal C as its frequency shifter instead of the RWP in Fig. 1(a). FM, frequency multiplier; BP, bandpass filter; PM, phase meter

enter the optical path below the dotted line through beam splitter BS. In the same way, the counterclockwise directional (CCW) wave entering fiber at end B comes out at end A as a vertical polarized light and also enters the optical path below the dotted line through BS. It is obvious that the CW wave and CCW wave entering the optical path below the dotted line remain horizontal and vertical linearly polarized beams, respectively, whose phase difference depends on the Sagnac effect at reciprocity. Both the linearly polarized beams are transformed into left and right circularly polarized beams through a  $\lambda/4$  quarter-wave plate placed at  $45^\circ$  in the horizontal direction, after that they go through a wave plate with phase delay  $\delta$  which can be expressed as

$$\left\{ \begin{aligned} \begin{bmatrix} V_{\omega} \\ V_{-\omega} \end{bmatrix} &= \frac{a}{\sqrt{2}} \begin{bmatrix} \cos \varphi & -\sin \varphi \\ \sin \varphi & \cos \varphi \end{bmatrix} \begin{bmatrix} 1 & 0 \\ 0 & e^{i\delta} \end{bmatrix} \begin{bmatrix} \cos \varphi & \sin \varphi \\ -\sin \varphi & \cos \varphi \end{bmatrix} \begin{bmatrix} 1 \\ -i \end{bmatrix} e^{i(\omega t + \varphi)} \\ \begin{bmatrix} V_{\omega} \\ V_{-\omega} \end{bmatrix} &= \frac{b}{\sqrt{2}} \begin{bmatrix} \cos \varphi & -\sin \varphi \\ \sin \varphi & \cos \varphi \end{bmatrix} \begin{bmatrix} 1 & 0 \\ 0 & e^{i\delta} \end{bmatrix} \begin{bmatrix} \cos \varphi & \sin \varphi \\ -\sin \varphi & \cos \varphi \end{bmatrix} \begin{bmatrix} -i \\ 1 \end{bmatrix} e^{i\omega t} \end{aligned} \right\} \quad (1)$$

where  $V_{\omega}, V_{-\omega}$  and  $V_{\omega}, V_{-\omega}$  are the field components of polarized beams in left and right figures, respectively;  $\varphi$  is the simultaneous azimuth of the wave plate;  $\alpha$  is the phase difference between two waves, the so-called Sagnac phase;  $a$  and  $b$  are amplitudes of two waves.

Through analyzer  $P_2$  with the azimuth  $\psi$ , the two waves expressed in Equation (1) reach detector D with their light intensity expressed as

$$I = |(V_{\infty} + V_{re}) \cos \psi + (V_{\infty} + V_{rs}) \sin \psi|^2. \quad (2)$$

Combining the above two equations and simplifying them yields

$$\left. \begin{aligned} I &= I_1 + I_2 + I_3, \\ I_1 &= \frac{1}{2} [a^2 + b^2 - ab(1 + \cos \delta) \sin(a - 2\psi)], \\ I_2 &= \frac{1}{2} (a^2 - b^2) \sin \delta \sin(2\varphi - 2\psi), \\ I_3 &= \frac{1}{2} ab(1 - \cos \delta) \sin(4\varphi - a - 2\psi). \end{aligned} \right\} \quad (3)$$

When the wave plate rotates with the angular frequency  $(\omega_m/2)$  that is  $2\varphi = \omega_m t$ , the  $I_1$  in Equation (3) corresponds to the direct-current component of light intensity, while  $I_2$  and  $I_3$  correspond to alternating-current components of light intensity with their frequencies being the fundamental and multiple of  $\omega_m$ , respectively. Due to equation (3) the phase difference  $\alpha$  to be measured has moved from the light frequency phase to the term of low frequency  $2\omega_m$ , it can be obtained by phase measurement of multiple frequency terms to determine the rotation rate of the gyroscope. The phase measurement is amplitude-independent, so there is no special range for value of  $\delta$  provided the amplitude  $I_3$  is sufficiently large.

### 3. Electro-optic frequency shifter (electro-optic frequency modulator)

This paper discusses a series of problems in replacing an electro-optic frequency shifter for mechanical rotating wave plate to eliminate complicated transmission. Following the analysis in literature [9] we emitted the light along the triad axis of a  $\text{LiNbO}_3$  crystal, the z axis. Due to the symmetry of the crystal, the refracting power ellipse without an external electric field shows a circle projection on the cross section perpendicular to the triad axis. That means that the crystal has no eigen birefringence along the triad axis direction. Applying an electric field  $E_x = E_m \sin \omega_m t$  and  $E_y = E_m \sin \omega_m t$ , along the directions perpendicular to the triad axis (the X, Y directions), the refracting power ellipse shows the ellipse projection on the XY cross section which has furthermore been proved to rotate with the angular frequency  $(\omega_m/2)$

in the direction opposite to the rotation direction of the external electric field. This indicates that the  $\text{LiNbO}_3$  crystal plays the same role in the rotating external field as a mechanical rotating wave plate does. Using equations related to the photoelectric effect, the phase delay difference  $\delta$  of this electro-optical crystal equivalent to rotating wave plate can be determined as

$$\delta = 2\pi l \bar{r} E_m n_0^3 / \lambda, \quad \bar{r} = \sqrt{r_{11}^2 + r_{22}^2}, \quad (4)$$

where  $l$  is the thickness of the crystal,  $r_{11}$  and  $r_{22}$  are the electro-optical coefficient of the crystal. In case of  $\text{LiNbO}_3$ ,  $r_{11} = 0$ , so  $\bar{r} = r_{22}$ . As shown in Figure 1(b), we set on the frequency shifter,  $\text{LiNbO}_3$  crystal, two pairs of electrodes perpendicular to each other which allow the simultaneous application of the transverse electric field  $E_x$  and the longitudinal electric field  $E_y$ . Replacing such an electro-optic frequency shifter for a mechanical rotating wave plate, we made the purely electronic device--heterodyne optic-fiber gyroscope.

#### 4. Experiment and result analysis

There has been no report of measuring the optical frequency phase by an electro-optic frequency shifter so far. Our experiment contains two procedures.

The first one is to check the accuracy in measurements of the phase difference between left and right circularly polarized beams by applying an electro-optic frequency shifter to heterodyne interference system. The experiment set-up is shown in Figure 2 where the polarization direction of the linearly polarized beam output from the laser can be changed by changing the azimuth of the  $(\lambda/2)$  halfway plate. Due to the behavior of the polarized light, linearly polarized light is known as the superposition of left and right circularly polarized beams with the same amplitude and a fixed phase difference. A given change in azimuth of linearly polarized beams corresponds to a certain change in phase difference between two circularly polarized beams. Therefore, any given phase difference between two circularly polarized beams



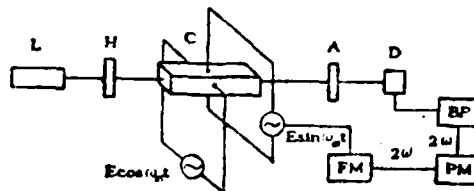


Fig. 2 Experimental set-up of the  $\text{LiNbO}_3$  electro-optic frequency shifter. L, He-Ne laser; H, halfwave plate; C,  $\text{LiNbO}_3$  crystal; A, analyzer; D, detector; BP, bandpass filter; FM, frequency multiplier; PM, phase meter

can be achieved by changing the azimuth of the  $(\lambda/2)$  halfwave plate. The frequency of the external electric field in our experiment is 1 kHz. From equation (3) the phase to be measured has been included in the term of signal light intensity  $I_3$  with  $4\varphi = 2\omega_e t$ , that is,  $I_3$  is the term for 2 kHz frequency. It has to be noted that a change of  $1^\circ$  in the  $(\lambda/2)$  halfwave plate azimuth corresponds to the change of  $4^\circ$  in the phase difference between two circularly polarized beams. Figure 3 shows the experimental results of phase measurements of heterodyne interference systems using  $\text{LiNbO}_3$  crystal electro-optic frequency shifters. Its curve shows the relation between the measured phase and azimuth of the  $(\lambda/2)$  halfwave plate. The result shows that the application of a  $\text{LiNbO}_3$  crystal electro-optic frequency shifter gives satisfactory accuracy in phase measurement and good linearity. In our experiment this accuracy depends on the reading accuracy of  $(\lambda/2)$  halfwave plate azimuth.

Later, we did experiments on actual application of  $\text{LiNbO}_3$  crystal electro-optic frequency shifter to a heterodyne gyroscope described in Section 2. The experiment set-up is shown in Figure 1 where Figure 1(a) is the fundamental optical path but its mechanical rotating wave plate is replaced by  $\text{LiNbO}_3$  crystal electro-optic frequency shifter in Figure 1(b). Two transverse electric fields being applied to  $\text{LiNbO}_3$  crystals differ  $90^\circ$  in phase and they have equal amplitude just the same as in the earlier experiment. The bandpass filter BP selects the 2 kHz component from the output of detector D and delivers it to

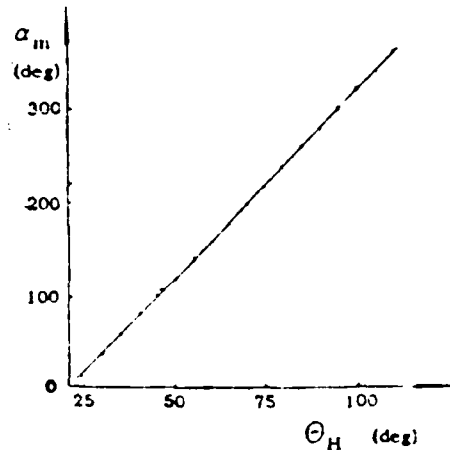


Fig. 3 Relation between the azimuth reading  $\Theta_H$  of the halfwave plate  $H$  and the phase  $\alpha_m$  measured by the phasemeter

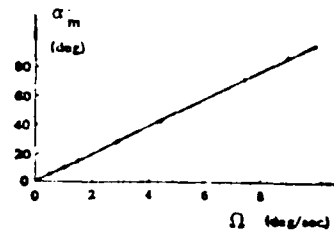


Fig. 4 Measured phase value  $\alpha_m$  versus the rotating rate  $\Omega$  of the gyroscope. The solid line denotes the ideal line, the dots indicate measured values

phasemeter PM for signal phase measurement. Frequency multiplier FM multiplies the frequency of the modulation signal from a single source and delivers it to PM as the phase measurement reference. Figure 4 shows the relation between the measured Signac phase value and the rotating rate of a heterodyne fiber-optic gyroscope. The result shows good linearity of the scale factor of the system. In our elementary experiment, we did not apply a space filter which ensures high reciprocity of the optical path of the system. For future experiments, we plan to add a space filter and micro-optical device in order to reduce zero drift and to make the system smaller-sized.

## 5. Conclusion

(1) This paper introduces the application of rotating techniques to direct-current detection of fiber-optic gyroscopes with highly birefringent fibers resulting in a novel heterodyne optic-fiber gyroscope. This method has the advantage of improving reciprocity of the optic path and no need of using acousto-optic frequency shifters in comparison to ordinary heterodyne fiber-optic gyroscopes. Besides, the heterodyne detection of this system is free from direct-current drift in electronics and shows good linearity of the scale factor within a great dynamic range.

(2) Concerning problems caused by mechanical complexity of rotating wave plate techniques and mechanical noise, we designed a  $\text{LiNbO}_3$  crystal electro-optic frequency shifter and replaced it for the earlier mentioned mechanical rotating plate to construct a heterodyne gyroscope system which is purely solid and purely electronic.

(3) Our experimental result shows satisfactory accuracy in a measurement of the heterodyne interference system with an electro-optic frequency shifter. The experiment of applying a  $\text{LiNbO}_3$  crystal frequency shifter to the heterodyne optic-fiber gyroscope described in this paper shows good linearity of the scale factor of the system.

## References

- [1] B. Colshaw, I. P. Giles, *IEEE J. Quantum Electron.*, 1982, QE-18, No. 4 (Apr), 696.
- [2] K. Houta et al.; *Opt. Lett.*, 1982, 7, No. 7 (Jul), 331.
- [3] D. A. Jackson et al.; *Electron. Lett.*, 1984, 20, No. 10 (May), 399.
- [4] R. Crane; *Appl. Opt.*, 1969, 8, 338.
- [5] G. E. Sommargren; *J. Opt. Soc. Am.*, 1975, 65, 960.
- [6] R. N. Shyam, J. O. Wyant; *Appl. Opt.*, 1978, 17, 3034.
- [7] H. Z. Hu; *Appl. Opt.*, 1983, 22, No. 12 (Dec), 2052.
- [8] I. P. Kaminsor, E. H. Turner; *Appl. Opt.*, 1986, 25, No. 10 (Oct), 73.
- [9] C. F. Buhrer et al.; *Appl. Phys. Lett.*, 1982, 41, No. 1, 46.
- [10] G. L. Rogers; *Noncoherent Optical Processing*, (John Wiley & Sons, Inc., New York, 1977).

DISTRIBUTION LIST  
DISTRIBUTION DIRECT TO RECIPIENT

<u>ORGANIZATION</u>	<u>MICROFICHE</u>
A205 DMAHTC	1
C509 BALLISTIC RES LAB	1
C510 R&T LABS/AVEADCOM	1
C513 ARRADCOM	1
C535 AVRADCOM/TSARCOM	1
C539 TRASANA	1
C591 FSTC	4
C619 MIA REDSTONE	1
DOOS MISC	1
E053 HQ USAF/INET	1
E404 AEDC/DOF	1
E408 AFWL	1
E410 AD, IND	1
F429 SD/IND	1
P005 DOE/ISA/DDI	1
P050 CIA/OCB ADT SD	2
AFIT LEE	2
FTD	
CCV	1
MIA/PHS	1
LLVL/COM 1-389	1
NASA/NST-44	1
NSA/TS13 TPL	2
ASD/FTD/TOLA	2
FSL/NIX-3	1
NCOIC/OIC-9	

**BEST  
AVAILABLE COPY**